

Compensation of loss in propagating surface plasmon polariton by gain in adjacent dielectric medium

M. A. Noginov^{1*}, V. A. Podolskiy², G. Zhu¹, M. Mayy¹, M. Bahoura¹, J. A. Adegoke¹,
B. A. Ritzo³, K. Reynolds¹

¹ Center for Materials Research, Norfolk State University, Norfolk, VA 23504

² Department of Physics, Oregon State University, Corvallis, OR 97331-6507

³ Summer Research Program, Center for Materials Research, Norfolk State University, Norfolk, VA 23504
mnoginov@nsu.edu

Abstract: We report the suppression of loss of surface plasmon polariton propagating at the interface between silver film and optically pumped polymer with dye. The large magnitude of the effect enables a variety of applications of ‘active’ nanoplasmonics. The experimental study is accompanied by the analytical description of the phenomenon. In particular, we resolve the controversy regarding the direction of the wavevector of a wave with a strong evanescent component in an active medium.

©2008 Optical Society of America

OCIS codes: (240.6680) Surface plasmons; (240.6690) Surface waves; (260.3910) Metal optics; (350.3618) Left-handed materials.

References

1. R. H. Ritchie, “Surface plasmons in solids,” *Surf. Sci.* **34**, 1-19 (1973).
2. M. Fleischmann, P. J. Hendra, A. J. McQuillan, “Raman spectra of pyridine adsorbed at a silver electrode,” *Chem. Phys. Lett.* **26**, 163-166 (1974).
3. M. Moskovits, “Surface-enhanced spectroscopy,” *Rev. Mod. Phys.* **57**, 783-826 (1985).
4. H. Raether, *Surface plasmons on smooth and rough surfaces and on gratings*, (Springer-Verlag, Berlin, 1988).
5. K. Kneipp, Y. Wang, H. Kneipp, L. T. Perelman, I. Itzkan, R. R. Dasari, and M. S. Feld, “Single molecule detection using surface-enhanced Raman scattering (SERS),” *Phys. Rev. Lett.* **78**, 1667-1670 (1997).
6. S. Nie and S. R. Emory, “Probing single molecules and single nanoparticles by surface-enhanced Raman scattering,” *Science* **275**, 1102-1104 (1997).
7. H. F. Ghaemi, Tineke Thio, D. E. Grupp, T. W. Ebbesen, H. J. Lezec, “Surface plasmons enhance optical transmission through subwavelength holes,” *Phys. Rev. B* **58**, 6779-6782 (1998).
8. V. A. Podolskiy, A. K. Sarychev and V. M. Shalaev, “Plasmon modes in metal nanowires and left-hand materials,” *J. Nonlinear Opt. Phys. Mater.* **11**, 65-74 (2002).
9. H. Shin and S. Fan, “All-angle negative refraction for surface plasmon waves using a metal-dielectric-metal structure,” *Phys. Rev. Lett.* **96**, 073907 (2006).
10. V. M. Shalaev, W. Cai, U. Chettiar, H.-K. Yuan, A. K. Sarychev, V. P. Drachev and A. V. Kildishev, “Negative Index of Refraction in Optical Metamaterials,” *Opt. Lett.* **30**, 3356-3358 (2005).
11. G. Dolling, C. Enkrich, M. Wegener, C. M. Soukoulis, and S. Linden, “Simultaneous negative phase and group velocity of light in a metamaterial,” *Science* **312**, 892-894 (2006).
12. A. Alu and N. Engheta, “Optical nanotransmission lines: synthesis of planar left-handed metamaterials in the infrared and visible regimes,” *J. Opt. Soc. Am. B* **23**, 571-583 (2006).
13. S. I. Bozhevolnyi, V. S. Volkov and K. Leosson, “Localization and waveguiding of surface plasmon polaritons in random nanostructures,” *Phys. Rev. Lett.* **89**, 186801 (2002).
14. A. Boltasseva, S. I. Bozhevolnyi, T. Søndergaard, T. Nikolajsen and L. Kristjan, “Compact Z-add-drop wavelength filters for long-range surface plasmon polaritons,” *Opt. Express* **13**, 4237-4243 (2005).
15. S. A. Maier, P. G. Kik, H. A. Atwater, S. Meltzer, E. Harel, B. E. Koel, and A. A. G. Requicha, “Local detection of electromagnetic energy transport below the diffraction limit in metal nanoparticle plasmon waveguides,” *Nature Materials* **2**, 229-232 (2003).
16. A. Karalis, E. Lidorikis, M. Ibanescu, J. D. Joannopoulos and S. Marin, “Surface-plasmon-assisted guiding of broadband slow and subwavelength light in air,” *Phys. Rev. Lett.* **95**, 063901 (2005).

17. M. Stockman, "Nanofocusing of optical energy in tapered plasmonic waveguides," *Phys. Rev. Lett.* **93**, 137404 (2004).
18. C. Sirtori, C. Gmachl, F. Capasso, J. Faist, D. L. Sivco, A. L. Hutchinson, and A. Y. Cho, "Long-wavelength ($\lambda \approx 8\text{--}11.5\ \mu\text{m}$) semiconductor lasers with waveguides based on surface plasmons," *Opt. Lett.* **23**, 1366-1368 (1998).
19. M. A. Noginov, G. Zhu, M. Bahoura, J. Adegoke, C. E. Small, B. A. Ritzo, V. P. Drachev, and V. M. Shalaev, "Enhancement of surface plasmons in an Ag aggregate by optical gain in a dielectric medium", *Opt. Lett.* **31**, 3022-3024 (2006).
20. J. Seidel, S. Grafstroem and L. Eng, "Stimulated emission of surface plasmons at the interface between a silver film and an optically pumped dye solution," *Phys. Rev. Lett.* **94**, 177401 (2005).
21. G. A. Plotz, H. J. Simon and J. M. Tucciarone, "Enhanced total reflection with surface plasmons," *J. Opt. Soc. Am.* **69**, 419-421 (1979).
22. A. N. Sudarkin and P. A. Demkovich, "Excitation of surface electromagnetic waves on the boundary of a metal with an amplifying medium," *Sov. Phys. Tech. Phys.* **34**, 764-766 (1989).
23. I. Avrutsky, "Surface plasmons at nanoscale relief gratings between a metal and a dielectric medium with optical gain", *Phys. Rev. B* **70**, 155416 (2004).
24. M. P. Nezhad, K. Tetz and Y. Fainman, "Gain assisted propagation of surface plasmon polaritons on planar metallic waveguides," *Opt. Express* **12**, 4072-4079 (2004).
25. A. A. Gomyadinov and V. A. Podolskiy, "Gain-assisted slow to superluminal group velocity manipulation in nano-waveguides," *Phys. Rev. Lett.* **97**, 223902 (2006).
26. N. M. Lawandy, "Localized surface plasmon singularities in amplifying media," *Appl. Phys. Lett.* **85**, 5040-5042 (2004).
27. D. Bergman and M. Stockman, "Surface Plasmon Amplification by Stimulated Emission of Radiation: quantum generation of coherent Surface plasmons in nanosystems," *Phys. Rev. Lett.* **90**, 027402 (2003).
28. Y. Chen, P. Fisher and F. W. Wise, "Negative refraction at optical frequencies in nonmagnetic two-component molecular media," *Phys. Rev. Lett.* **95**, 067402 (2005).
29. Y. Chen, P. Fisher and F. W. Wise, "Chen, Fischer, and Wise reply", *Phys. Rev. Lett.* **96**, 159702 (2006).
30. T. Mackay and A. Lakhtakia, Comment on "negative refraction at optical frequencies in nonmagnetic two-component molecular media", *Phys. Rev. Lett.* **96**, 159701 (2006).
31. V. G. Veselago, "The electrodynamics of substances with simultaneously negative values of ϵ and μ ," *Soviet Physics Uspekhi* **10**, 509-514 (1968).
32. R. W. Ziolkowski, E. Heyman, "Wave propagation in media having negative permittivity and permeability," *Phys. Rev. E* **64**, 056625 (2001).
33. L. D. Landau, E. M. Lifshitz, *Course of theoretical physics*, vol.8, ch.86. (Reed, Oxford, UK 1984).
34. B. Ya. Kogan, V. M. Volkov and S. A. Lebedev, "Superluminescence and generation of stimulated radiation under internal-reflection conditions," *JETP Lett.* **16**, 100-105 (1972).
35. I. Avrutsky, "Guided modes in a uniaxial multilayer," *J. Opt. Soc. A* **20**, 548-556 (2003).
36. X. Ma and C. Soukoulis, "Schrödinger equation with imaginary potential," *Physica B*, **296**, 107-111 (2001).
37. P. B. Johnson and R. W. Christy, "Optical constants of the noble metals," *Phys. Rev. B* **6**, 4370-4379 (1972).
38. K. Selanger, A. J. Falnes and T. Sikkeland, "Fluorescence lifetime studies of Rhodamine 6G in methanol," *J. Phys. Chem.* **81**, 1960-1963 (1977).

1. Introduction

Resonant oscillations of free electrons in metallic nanostructures, known as localized surface plasmons (SPs) [1-3], and their propagating counterparts – oscillations of electron density coupled to electromagnetic waves, known as surface plasmon polaritons (SPPs) [4], comprise a very hot topic in modern photonic research. Surface plasmons have been named an enabling mechanism in a number of unique optical phenomena, including surface-enhanced Raman spectroscopy [5,6], extraordinary optical transmission [7] and negative index of refraction [8-12]. They are broadly used in photonic and optoelectronic devices [13-18], including waveguides, couplers, splitters, add/drop filters, and quantum cascade lasers.

Many applications of surface plasmons suffer from damping caused by absorption in metals. The compensation of loss in *localized* SPs by optical gain in dielectric has been demonstrated in Ref. [19]. Here we report conquering the loss in *propagating* SPPs at the interface between silver film and optically pumped polymer with dye. In contrast to Ref. [20], where an elongation of the SPP propagation length caused by optical gain was infinitesimally small, the value of gain achieved in our experiments, $\approx 420\ \text{cm}^{-1}$, is sufficient to fully compensate SPP loss in high-quality silver films, thus enabling practical applications of a

broad range of low-loss and no-loss photonic metamaterials.

Over the years, several proposals to compensate loss by incorporating optical gain into plasmonic systems have been made. Theoretically, field-matching approach was employed to calculate the reflectivity at surface plasmon excitation [21]; the authors of [22] proposed that the optical gain in a dielectric medium can elongate the SPP's propagation length; gain-assisted excitation of resonant SPPs was predicted in [23]; SPP propagation in active waveguides was studied in [24]; and the group velocity modulation of SPPs in nano-waveguides was discussed in [25]. Localized SP resonance in metallic nanospheres was predicted to exhibit a singularity when the surrounding dielectric medium had a critical value of optical gain [26]. A relevant excitation of localized plasmon fields in active nanosystems using surface plasmon amplification by stimulated emission of radiation (SPASER) was proposed in [27].

2. Setup geometry and theoretical model

In this work, the experimental setup consisted of a glass prism with the dielectric permittivity $\epsilon_0=n_0^2$, a metallic film with the complex dielectric constant ϵ_l and thickness d_l , and a layer of dielectric medium characterized by the permittivity ϵ_2 , Fig. 1(a).

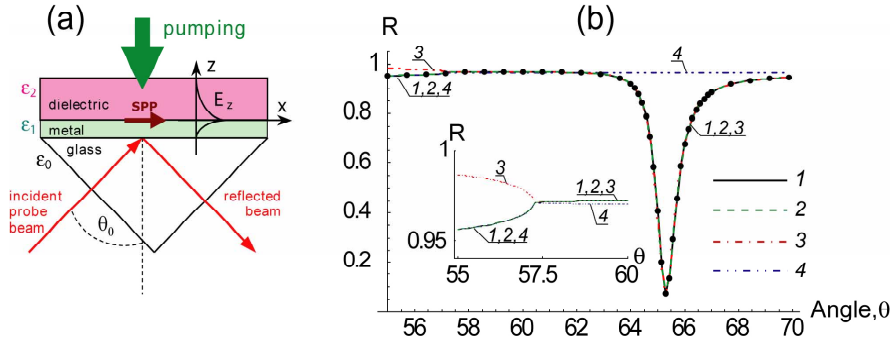


Fig. 1. (a) Schematic of SPP excitation. (b) Reflectivity R as a function of angle θ . Traces – solutions of exact Eq. (3). Dots – solution of approximate Eq. (5). For all data sets: $\epsilon_l = -15.584 + 0.424i$, $d_l = 60$ nm. Trace 1: dielectric with very small loss, $\epsilon_2 = 2.25 + 10^{-5}i$. Traces 2-4: dielectric with very small gain, $\epsilon_2 = 2.25 - 10^{-5}i$. Trace 2 and dots: cut of the complex plane along negative imaginary axis (correct; nearly overlaps with trace 1; no discontinuity at the transition from small loss to small gain). Trace 3: cut along positive real axis (yields incorrect predictions for incident angles below total internal reflection). Trace 4: cut along negative real axis (yields incorrect predictions for incident angles above total internal reflection).

The SPP propagates at the boundary between media 1 and 2, and has the wavevector [4]

$$k_x^0 = \frac{\omega}{c} \sqrt{\frac{\epsilon_1 \epsilon_2}{\epsilon_1 + \epsilon_2}}, \quad (1)$$

where ω is the oscillation frequency and c is the speed of light. SPP can be excited by a p polarized light falling on the metallic film at the critical angle θ_0 , such that the projection of its wave vector to the axis x ,

$$k_x(\theta) = (\omega/c)n_0 \sin \theta_0, \quad (2)$$

is equal to $\text{Re}(k_x^0)$. At this resonant condition, the energy of incident light is transferred to the SPP, yielding a minimum (dip) in the angular dependence of the reflectivity $R(\theta)$ [4]:

$$R(\theta) = \frac{\left| r_{01} + r_{12} \exp(2ik_{z1}d_1) \right|^2}{\left| 1 + r_{01}r_{12} \exp(2ik_{z1}d_1) \right|^2}, \quad (3)$$

where $r_{ik} = (k_{zi}\epsilon_k - k_{zk}\epsilon_i) / (k_{zi}\epsilon_k + k_{zk}\epsilon_i)$ and

$$k_{zi} = \pm \sqrt{\epsilon_i \left(\frac{\omega}{c} \right)^2 - k_x(\theta)^2}, \quad i = 0, 1, 2. \quad (4)$$

The parameter $k_z c / \omega$ defines the field distribution along the z direction. Its real part can be associated with a tilt of phase-fronts of the waves propagating in the media [24], and is often discussed in the context of positive vs. negative refractive index materials (see also Refs. [8-12,28-30]), while its imaginary part defines the wave attenuation or growth. Note that from the mathematical point of view, the parameter k_z is defined by the multi-valued function (square root). Hence, to adequately describe the optical properties of the system, it is necessary to identify the proper cut in the complex plane describing the values of k_z^2 .

The sign of the square root in Eq. (4) does not follow from Maxwell's equations alone and must be selected to enforce the physical energy propagation [30-33]. In dielectrics excited in total internal reflection geometry, as well as in metals and other media with $\text{Re}[k_z^2] < 0$, which do not support propagating waves, the field must exponentially decay away from the source. Hence $[k_z]'$ should be always positive regardless of the sign of ϵ'' . (Here and below single $[']$ and double $['']$ primes stand for real and imaginary parts of complex numbers, and $e^{-i\omega t}$ time-dependence is assumed.) For other systems, the sign selection in Eq. (4) should enforce the propagation of energy away from the source, corresponding to wave decay in systems with loss ($\epsilon'' > 0$) and the wave growth in materials with gain ($\epsilon'' < 0$) [30]. This selection of the sign can be achieved by the cut of the k_z^2 complex plane along the negative imaginary axis (meaning that the phase of complex numbers is defined between $-1/2\pi$ and $3/2\pi$).

Although such cut of the complex plane is different from other previously proposed cuts along the positive [28,29] or negative [8-12,30] real axes, our sign selection is the only one satisfying the physical solutions of Maxwell equations; it is also consistent with previous results on reflection from passive systems, on gain-assisted reflection enhancement, predictions of gain-assisted SPP behavior [21-23,34], and the experimental data presented below. The implications of selecting different signs of k_{z2} are shown in Fig.1(b).

Active media excited above the angle of total internal reflection, as well as the materials with $\epsilon' < 0$ and $\epsilon'' < 0$ formally fall under negative index materials category, since $\text{Re}(k_z') < 0$. However, since $|k_z''|$ in this case is greater than $|k_z'|$, the wave experiences very large attenuation (in the presence of gain), which in contrast to claims of [28], makes the material unsuitable for superlens and other proposed applications of NIMs [8-12].

In the limit of small plasmonic loss/gain, when the decay length of SPP, L , is much greater than $2\pi/k_x^{(0)}$, and in the vicinity of θ_0 , Eq. (3) can be simplified, revealing the physics behind the gain-assisted plasmonic loss compensation:

$$R(\theta) \approx |r_{01}^0|^2 \left[1 - \frac{4\gamma_i\gamma_r + \delta(\theta)}{(k_x - k_x^0 - \Delta k_x^0)^2 + (\gamma_i + \gamma_r)^2} \right], \quad (5)$$

where $r_{01}^0 = r_{01}(\theta_0)$, $\delta(\theta) = 4(k_x - k_x^0 - \Delta k_x^0) \text{Im}(r_0) \text{Im}(e^{i2k_z^0 d_1}) / \xi$, and

$$\xi = \frac{c(\epsilon_2' - \epsilon_1')}{2\omega} \left(\frac{\epsilon_2' + \epsilon_1'}{\epsilon_2'\epsilon_1'} \right)^{3/2}.$$

The shape of $R(\theta)$ is dominated by the Lorentzian term in Eq. (5). Its width is determined by the propagation length of SPP,

$$L = [2(\gamma_i + \gamma_r)]^{-1}, \quad (6)$$

which, in turn, is defined by the sum of the *internal* (or propagation) loss

$$\gamma_i = k_x^{0''} = \frac{\omega}{2c} \left(\frac{\epsilon_1' \epsilon_2'}{\epsilon_1' + \epsilon_2'} \right)^{3/2} \left(\frac{\epsilon_1''}{\epsilon_1'^2} + \frac{\epsilon_2''}{\epsilon_2'^2} \right). \quad (7)$$

and the *radiation* loss caused by SPP leakage into the prism,

$$\gamma_r = \text{Im} \left(r_{01} e^{i2k_z^0 d_1} \right) / \xi. \quad (8)$$

The radiation loss also leads to the shift of the extremum of the Lorentzian profile from its resonant position k_x^0 ,

$$\Delta k_x^0 = \text{Re} \left(r_{01} e^{i2k_z^0 d_1} \right) / \xi. \quad (9)$$

The term δ in Eq. (5) results in the asymmetry of $R(\theta)$.

The excellent agreement between exact Eq. (3) and approximate Eq. (5) for 60 nm-thick silver film is shown in Fig. 1(b). The behavior of $R(\theta)$ as a function of gain is illustrated in Fig. 2 and is described below. To verify the accuracy of Eq. (6), we modeled the experimental setup, where plasmonic nanolayer system was irradiated by a beam of finite angular size by using a transfer matrix technique [35]. Results of these simulations, along with the agreement between the propagation length extracted from numerical solutions and Eq.(6) are shown in Fig. 3.

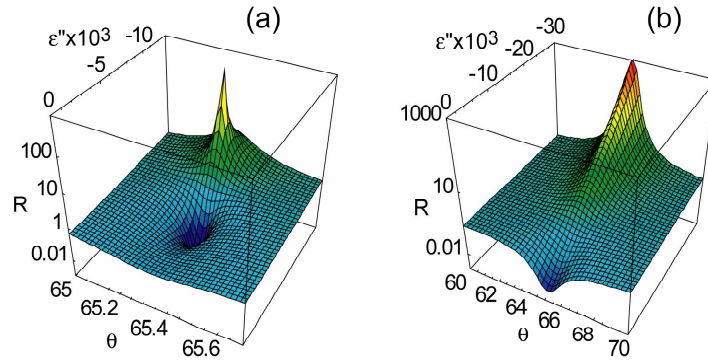


Fig. 2. Reflectivity R [Eq.(5)] of the three-layer system depicted in Fig. 1(a) as a function of angle θ and gain (given by imaginary part of ϵ_2); (a) $d_f=70$ nm, (b) $d_f=39$ nm.

The gain in the medium reduces internal loss γ_i of SPP, Eq. 7. In reasonably thick metallic films (where $\gamma_i > \gamma_r$ in the absence of gain) the “dip” in the reflectivity profile R_{min} is reduced when gain is first added to the system, reaching $R_{min}=0$ at $\gamma_i \approx \gamma_r$ (Fig. 2(a)). With further increase of gain, γ_i becomes smaller than γ_r , leading to an increase of R_{min} . The resonant value of R is equal to unity when *internal* loss is completely compensated by gain ($\gamma_i=0$) at

$$\epsilon_2'' = - \frac{\epsilon_1'' \epsilon_2'^2}{\epsilon_1'^2}. \quad (10)$$

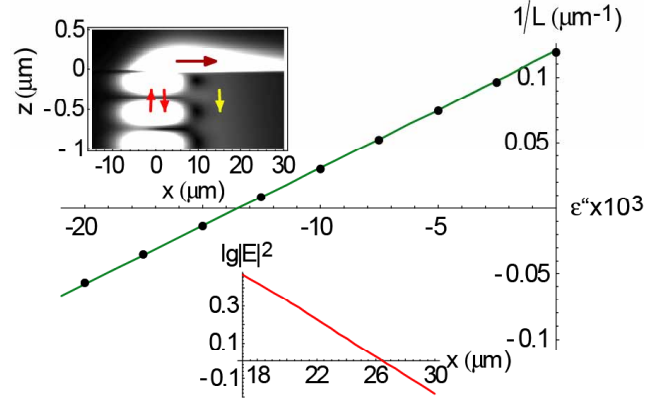


Fig. 3. Inverse propagation length of SPP, L^{-1} , in the system depicted in Fig.1(a) as a function of gain in dielectric, ϵ'' . Solid line – solution of Eq. (6), dots – exact numerical solution of Maxwell equations. Top inset: intensity distribution across the system; the arrows represent the directions of excitation beam; reflected beam; SPP propagation; and radiative SPP decay; angle of incidence: 65° (note different scale in x and z directions). Bottom inset: Exponential decay of the SPP wave intensity $|E|^2$ (shown in the top inset) along the propagation in the x direction.

In the vicinity of $\gamma_i=0$, the reflectivity profile is dominated by the asymmetric term δ . When gain is increased to even higher values, γ_i becomes negative and the dip in the reflectivity profile converts into a peak, consistent with predictions of Refs. [21,22]. The peak has a singularity when the gain compensates total SPP loss ($\gamma_i + \gamma_r = 0$). Past the singularity point, the system becomes unstable and cannot be described by stationary Eqs. (3-5) [36]. In thin metallic films (when $\gamma_i < \gamma_r$ at $\epsilon_2'' = 0$), the resonant value of R monotonically grows with the increase of gain, Fig. 2(b).

3. Experiment

Experimentally, SPPs were studied in the attenuated total internal reflection setup of Fig. 1(a). The 90° degree prism was made of glass with the index of refraction $n_0=1.784$. Metallic films were produced by evaporating 99.99% pure silver. Rhodamine 6G dye (R6G) and polymethyl methacrylate (PMMA) were dissolved in dichloromethane. The solutions were deposited to the surface of silver and dried to a film. The concentration of dye in dry PMMA was equal to 10 g/l (2.1×10^{-2} M) and the thickness of the polymer film was of the order of 10 μm .

The prism was mounted on a goniometer. The reflectivity R was probed with p polarized He-Ne laser beam at $\lambda=594$ nm. The reflected light was detected by a photomultiplier tube (PMT) connected to the integrating sphere, which was moved during the scan to follow the walk of the beam. The permittivity of metallic film was determined by fitting the experimental reflectivity profile $R(\theta)$ with Eq.(3), inset of Fig. 4(a).

In the measurements with optical gain, the R6G/PMMA film was pumped from the back side of the prism (Fig. 1(a)) with Q-switched pulses of the frequency doubled Nd:YAG laser ($\lambda=532$ nm, $t_{\text{pulse}}=10$ ns, repetition rate 10 Hz). The pumped spot, with the diameter of ~ 3 mm, completely overlapped the smaller spot of the He-Ne probe beam. Reflected He-Ne laser light was steered with the set of mirrors to the entrance slit of a monochromator, set at $\lambda=594$ nm, with PMT attached to the monochromator's exit slit. The large distance (~ 2 m) between the prism and the sub-millimeter (~ 200 μm) input slit of the monochromator provided for some spatial filtering of the reflected He-Ne laser light. Experimentally, we recorded reflectivity kinetics $R(\theta, t)$ under short-pulsed pumping at different incidence angles (Fig. 4(b)).

In samples with relatively thin (≈ 40 nm) metallic films, despite the spatial filtering, strong emission signal from the R6G-PMMA film was observed in the absence of He-Ne probe beam. We therefore performed two measurements of kinetics for each data point: one in the absence of the probe beam, and one in the presence of the beam. We then subtracted “emission background” (measured without He-Ne laser) from the combined reflectivity and emission signal. The kinetics measurements had a relatively large data scatter, which was partially due to the instability of the Nd:YAG laser.

The results of the reflectivity measurements in the 39 nm silver film are summarized in Fig. 4(a). Two sets of data points correspond to the reflectivity without pumping (measured in flat parts of the kinetics before the laser pulse) and with pumping (measured in the peaks of the kinetics). By dividing the values of R measured in the presence of gain by those without gain, we calculated the relative enhancement of the reflectivity signal to be as high as 280% – a significant improvement in comparison to Ref. [8], where the change of the reflectivity in the presence of gain did not exceed 0.001%. Fitting both reflectivity curves with Eq. (3) and known $\epsilon_l = -15$, $\epsilon_l' = 0.85$ and $\epsilon_2' = n_2^2 = 2.25$, yields $\epsilon_2'' \approx -0.006$. This corresponds to the optical gain of 420 cm^{-1} (at $\lambda = 594 \text{ nm}$) and $\sim 35\%$ reduction in internal SPP loss. (Note that in Ref.

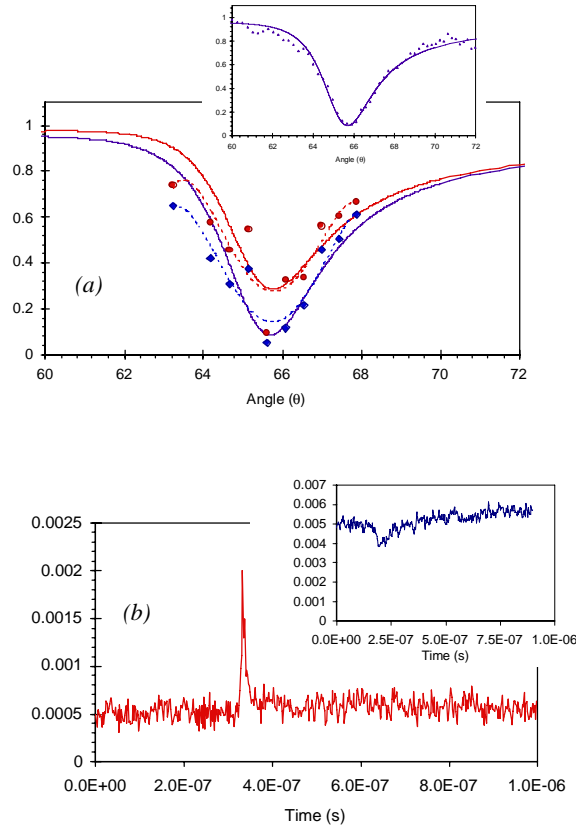


Fig. 4. (a) Reflectivity $R(\theta)$ measured without (diamonds) and with (circles) optical pumping in the glass-silver-R6G/PMMA structure. Dashed lines – guides for eye. Solid lines – fitting with Eq. (3) at $\epsilon_0' = n_0^2 = 1.784^2 = 3.183$, $\epsilon_0'' = 0$, $\epsilon_l' = -15$, $\epsilon_l'' = 0.85$, $d_l = 39 \text{ nm}$, $\epsilon_2' = n_2^2 = 1.5^2 = 2.25$, $\epsilon_2'' \approx 0$ (trace 1) and $\epsilon_2'' \approx -0.006$ (trace 2). Inset: Reflectivity $R(\theta)$ recorded in the same system without pumping (dots) and its fitting with Eq. (3) (solid line). (b) Reflectivity kinetics recorded under pumping. The angle θ corresponds to the minimum of the reflectivity; $d_l = 39 \text{ nm}$. Inset: Reflectivity kinetics recorded in a thick film ($d_l = 90 \text{ nm}$) shows a ‘dip’ at small values of gain.

[8], the concentration of dye molecules was equal to $N = 7 \times 10^{17} \text{ cm}^{-3}$ and the peak pumping density was equal to $P/S \sim 12 \text{ W/cm}^2$. The corresponding values in our work were $N \sim 1.2 \times 10^{22} \text{ cm}^{-3}$ and $P/S \sim 1.7 \times 10^7 \text{ W/cm}^2$. Although the optical gain in systems with SPPs and population inversion saturation is not directly proportional to the values above, it was orders of magnitude higher in our experiment than in Ref. [20]. This caused a dramatic difference between the results of the two works.)

In thicker silver films, calculations predict initial reduction of the minimal reflectivity $R(\theta)$ at small values of gain followed by its increase (after passing the minimum point $R=0$) at larger gains, Fig. 2(a). The reduction of R was experimentally observed in the 90 nm thick film, where instead of a peak in the reflectivity kinetics, we observed a dip, inset of Fig. 4(b).

For the silver film parameters measured in our experiment, Eq. (5) predicts complete compensation of *internal* SPP loss at optical gain of 1310 cm^{-1} . For better quality silver characterized by the dielectric constant of Ref. [37], the predicted critical gain is smaller, equal to 600 cm^{-1} . In addition, if a solution of R6G in methanol ($n=1.329$) is used instead of the R6G/PMMA film, then the critical value of gain is further reduced to 420 cm^{-1} . This is the value of gain achieved in our experiment. Thus, in principle, at the available gain, one can fully compensate the *internal* SPP loss in silver.

The radiation loss, which is significantly large in 39 nm silver film, becomes negligibly small at the thickness of metal exceeding $\sim 100 \text{ nm}$. Correspondingly, the demonstrated value of gain should be sufficient to compensate *total* SPP loss in thick silver films. In the experiment described above, the concentration of R6G molecules in the PMMA film was equal to $1.26 \times 10^{19} \text{ cm}^{-3}$ ($2.1 \times 10^{-2} \text{ M}$). Using the spectroscopic parameters known for R6G dye and neglecting any stimulated emission effects, one can estimate that 18 mJ laser pulses used in the experiment should excite more than 95% of all dye molecules. At the emission cross section equal to $2.7 \times 10^{-16} \text{ cm}^2$ at $\lambda=594 \text{ nm}$, this concentration of excited molecules corresponds to the gain of 3220 cm^{-1} . Nearly eight-fold difference between this value and the one obtained in our experiment is probably due to the combined effects of luminescence quenching of R6G occurring at high concentration of dye [38], and amplified spontaneous emission in photonic and SPP modes. The detailed study of the latter effect will be reported elsewhere.

Note that R6G dye molecules in PMMA photobleach with time. In line with Ref. [20], the longevity of the system can be improved by replacing the solid polymeric gain medium with a microfluidic flow cell with liquid dye solution.

4. Summary

In our study of the propagating surface plasmon polariton in the attenuated total reflection setup, we have established the relationship between (i) the gain in the dielectric adjacent to the metallic film, (ii) the *internal*, *radiative* and *total* losses, (iii) the propagation length of the SPP, and (iv) the shape of the experimentally measured reflectivity profile $R(\theta)$. We have experimentally demonstrated the optical gain in the dielectric (PMMA film with R6G dye) equal to 420 cm^{-1} . In the case of thick low-loss silver film [37] and low index dielectric, the demonstrated value of gain is sufficient for compensation of the total loss hindering the propagation of surface plasmon polariton.

Acknowledgments

The work was supported by the NSF PREM grant # DMR 0611430, the NSF CREST grant # HRD 0317722, the NSF NCN grant # EEC-0228390, the NSF grant #ECCS-0724763, the NASA URC grant # NCC3-1035, ONR, ARO/ARL and the Petroleum Research Fund. The authors cordially thank Vladimir M. Shalaev for useful discussions.